Laser and Particle Beams (2016), *34*, 655–662.

doi:10.1017/S0263034616000616

Emission spectra of noble gases and their mixtures under ion beam excitation

M.U. KHASENOV

National Laboratory Astana, Nazarbayev University, 53 Kabanbay Batyr Avenue, Astana 010000, Kazakhstan

(Received 3 July 2016; Accepted 5 September 2016)

Abstract

The luminescence spectra of noble gases and their binary mixtures were measured using heavy ion beam excitation from a DC-60 accelerator. Spectra were measured in the range of 200–975 nm; the gas spectra were dominated by lines of *p*–*s* and *d*–*p* atomic transitions; in neon and argon, lines from atomic oxygen, N_2, N_2^+, and OH radical bands were also observed. The ultraviolet region of the spectra was represented by a "third continuum" of noble gases. In krypton, the band of the KrO excimer molecule with a maximum at 557 nm was also observed. The maxima of the heteronuclear ionic molecules bands were located at wavelengths of 329 and 506 nm (Ar–Xe), 491 nm (Kr–Xe), and 642 nm (Ar–Kr). The relative intensities of the 2*p*–1*s* transitions of the noble gases atoms were measured and are discussed.

Keywords: Noble gas; Accelerator; Luminescence; Atomic transitions; Molecular bands

1. INTRODUCTION

Interest in studying the spectral–luminescent properties of low-temperature plasma excited by ionized radiation is because such plasma is an active medium of gas lasers using nuclear or beam pumping (Ulrich *et al.*, 2006; Mel'nikov *et al.*, 2015) and spontaneous emission sources (Prelas *et al.*, 1988; Ulrich, 2012) and is used in ionizing radiation detectors (Sakasai *et al.*, 1996). Although the luminescent properties of such plasma have been studied for more than 50 years (Bennet, 1962; De Young & Weaver, 1980; Mis'kevich, 1991), these studies cannot be considered as complete. Most of the research has been devoted to individual spectrum parts especially the ultraviolet (UV) spectrum. Part of the research was carried out previously when the line intensity could not be determined with sufficient accuracy.

Studies of the absolute line intensities of argon, krypton, and xenon in the range of 400–900 nm subject to excitation using $^3He(n,p)^3H$ nuclear reaction products are shown in (Boody & Prelas, 1993). The emission spectra of mixtures containing of the order of 1.3 kPa of argon, krypton, or xenon and 100–106 kPa ^3He have been studied, and such mixtures were concluded to have no obvious atomic lines in the Nd:YAG or Nd:glass absorption bands. The luminescence spectra of rare gases and their binary mixtures in the range of 350–875 and 740–1100 nm with excitation using uranium fission fragments were studied in (Gorbunov *et al.*, 2004; Abramov *et al.*, 2006).

In the present paper, we have studied the luminescence spectra of noble gases and their binary mixtures in the 200–975 nm range subject to excitation using heavy ion beams.

2. EXPERIMENTAL SETUP

The studies were carried out on an ion accelerator DC-60 (Gikal *et al.*, 2008; Zdorovets *et al.*, 2014). DC-60 accelerator is a dual cyclotron; multi-charged ions are produced in the Electron Cyclotron Resonance ion source and are transported by injection channel into the center of the cyclotron magnet, where main acceleration takes place. The main parameters of the accelerated ion beam were the following: ion type was from lithium to xenon, the ion energy varied from 0.5 to 1.75 MeV/nucleon. The intensity of ion beam varied from 10^{12} to 10^{14} particles/s depending on the type and energy of the ions. The ion impulse duration was several nanoseconds at an ion repetition rate of 1.84–4.22 MHz. Primarily argon ions were used as a source of ionization and excitation. The accelerated ion beam passed from an evacuated transportation channel through a 3-mm hole in the flange to the irradiation chamber (Fig. 1). The hole in the flange was closed using a 2-μm titanium foil membrane or a 2.5-μm-thick

Address correspondence and reprint requests to: M.U. Khasenov, National Laboratory Astana, Nazarbayev University, 53, Kabanbay Batyr Avenue, NLA, Astana 010000, Kazakhstan. E-mail: mendykhan.khassenov@nu.edu.kz

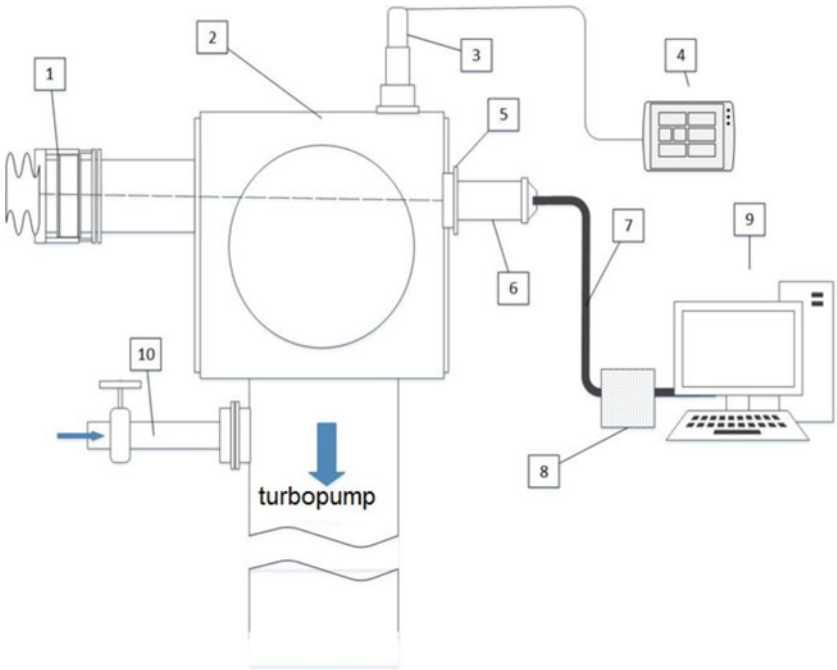

Fig. 1. Schematic representation of the installation: flange with Ti foil (1); irradiation chamber (2); pressure gauge (3); pressure controller (4); quartz window (5); collimator (6); fiber (7); spectrometer (8); PC (9); gas inlet valve (10).

Havar foil. The internal volume of the irradiation chamber was 34 liters ($380 \times 300 \times 300$ mm^3). The chamber was pumped out by turbomolecular pump up to vacuum 0.1 Pa before gas puffing. Gases were used with an impurity content of $<10^{-3}$%, and the whole system was flushed several times with the new gas. The gas pressure in the cell was measured using a capacitance diaphragm gauge (Agilent Technologies CDG-500) mounted on the top of the chamber.

The ions passed through the foil and ionized and excited the gas mixture in the irradiation chamber. The argon ion energy after the separation foil was approximately 55 MeV, the beam current was 20 nA, and the corresponding pump power of 80 kPa argon was $W \approx 3$ W/cm^3. The emerging light radiation passed through a quartz window and condenser lens made from fused silica and was focused on the optical fiber. The beam fell on a compact spectrometer (Ocean Optics QE65Pro) through the fiber, and the recorded spectrum was displayed on a computer. The relative spectral sensitivity of the system (quartz window, lens, optical fiber, and spectrometer) was on the range of 400–975 nm measured using a calibrated HL2000-CAL halogen lamp. In the UV region up to 210 nm, the quartz window transmission exceeded 50%, and the transmission boundary of the optic fiber and the lens was 190 nm. Some measurements are made using BK-7 glass lens with a diameter of 50.8 mm instead of a 25.4-mm quartz lens.

The distance from the separating flange to the output window was 500 mm. Runs of argon-40 ions with energy of 50 MeV in the gas under normal conditions range from 13 mm for xenon up to 114 mm for helium.

3. CONTINUUM AND MOLECULAR BANDS

An intense molecular band in the range of 200–400 nm with a maximum of approximately 260 nm was observed in the krypton spectrum (Fig. 2). This band is typically referred to as the third continuum of krypton (Boichenko *et al.*, 1993), and the origin of the third continuum was considered in (Boichenko *et al.*, 1999; Wieser *et al.*, 2000). The krypton atom line at $\lambda = 557$ nm was overlaid using a band of a KrO excimer molecule (McCusker, 1984), and the appearance of this band was, apparently, due to the presence of oxygen or water vapor in the krypton.

The band with a maximum at 230 nm corresponding to the third continuum in argon is weakly expressed. A strong band of 308 nm is connected due to transitions of the OH radical, and the bands of the second positive system of nitrogen were also observed (see Fig. 2).

The band of third continuum in xenon has several maxima: the main maxima at 270 and 390 nm (see Fig. 2). According to Wieser *et al.* (2000), these maxima correspond to different times of the decay of particles in the xenon plasma.

For neon, the maximum of the weak continuum occurs at approximately 280 nm, and there are bands of the second positive system of nitrogen and strong bands of the first negative system of nitrogen. According to Griegel *et al.* (1990) a maximum of the third continuum of neon is near 100 nm. The intensity of the 308 nm band of OH in neon was approximately three times less of this band intensity in argon. It should be noted that the water vapor content in neon (10^{-4}%) was three times less than in argon.

https://doi.org/10.1017/S0263034616000616 Published online by Cambridge University Press

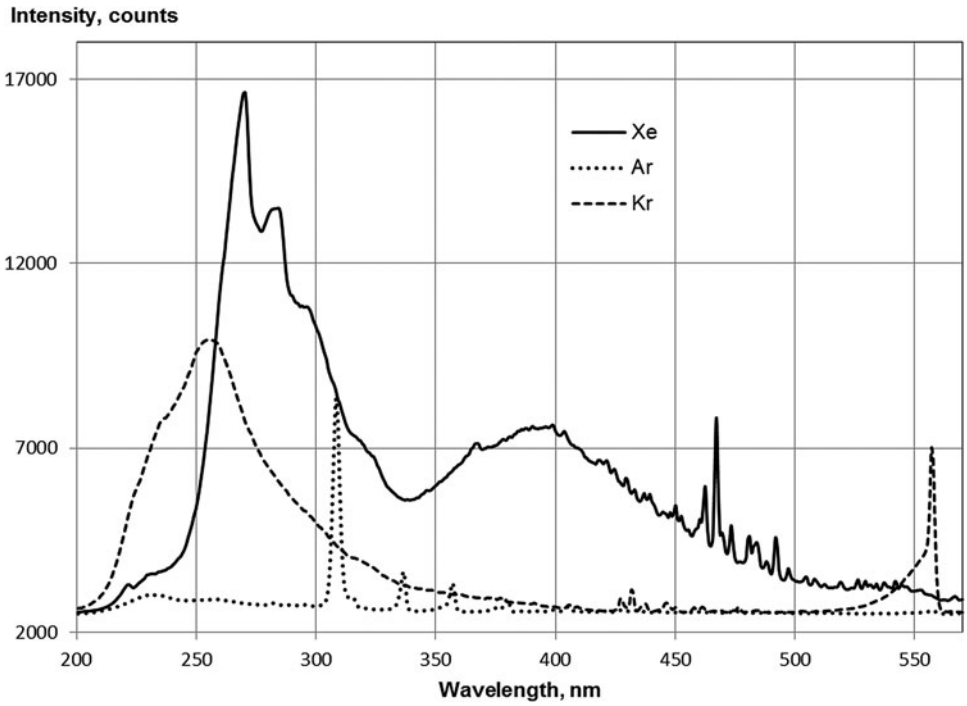

Fig. 2. Spectra of Ar(79.6 kPa), Kr(80.6 kPa), and Xe(30.7 kPa) under argon beam excitation in the range of 200–600 nm. Integration time of the spectrometer: 3*s*.

Figure 3 shows the emission spectra of the heteronuclear ionic molecules in the Ar–Xe, Ar–Kr, and Kr–Xe mixtures. The maxima of the bands of the heteronuclear ionic molecules are located at wavelengths of 329 and 506 nm (Ar–Xe), 491 nm (Kr–Xe), and 642 nm (Ar–Kr). Similar bands were previously observed in the electron beam excitation of the Ar–Xe, Ar–Kr (Kugler, 1964), and Kr–Xe mixtures (Friedl, 1959; Kugler, 1964). The molecular bands

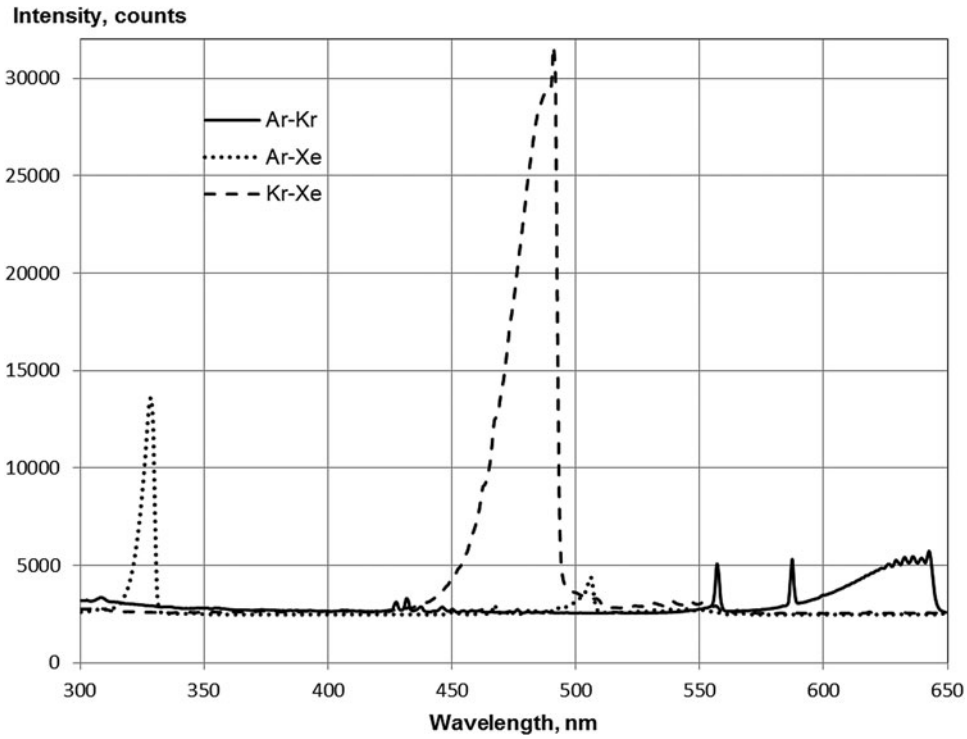

Fig. 3. Spectra of Ar(59.3 kPa)–Xe(6.7 kPa), Kr(53.3 kPa)–Xe(13.6 kPa) and Ar(53 kPa)–Kr(13.6 kPa) mixtures under argon beam excitation in the range of 300–650 nm. Integration time of spectrometer: 3*s* (Kr–Xe, Ar–Kr) and 1*s* (Ar–Xe).

https://doi.org/10.1017/S0263034616000616 Published online by Cambridge University Press

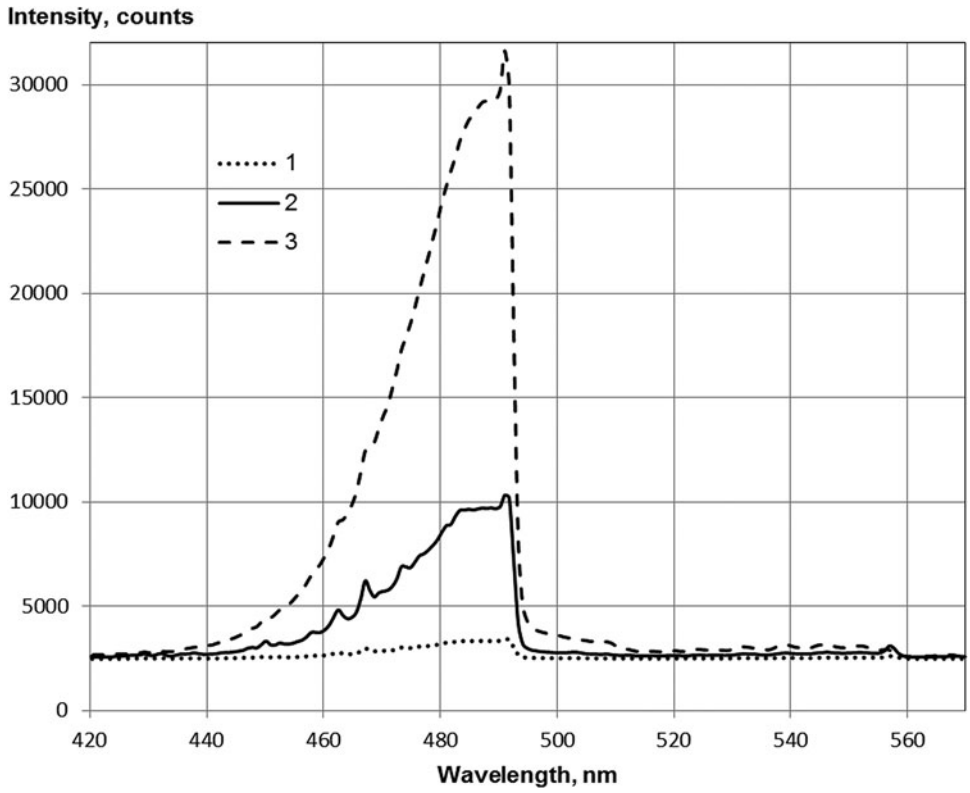

Fig. 4. Spectra of Kr–Xe under argon beam excitation in the range of 420–570 nm, a partial pressure of Kr of 53.3 kPa (1, 3) and 52 kPa (2) and a partial pressure of Xe of 0.67 kPa (1), 1.5 kPa (2), and 13.6 kPa (3).

observed in the emission spectra of the paired mixtures of the rare gases have been identified (Tanaka *et al.*, 1975) as the transitions between states of heteronuclear ionic molecules:

$$M^+N \rightarrow MN^+ + h\nu,$$

where the molecular states of M^+N asymptotically correspond to the $M^+ + N$ states, and the state of MN^+ to $M + N^+$. Here, M and N are atoms of rare gases, and N is the heavier atom. If, in the low-pressure plasma, an electrical discharge in paired mixtures of rare gases observed up to 5 of these bands (Tanaka *et al.*, 1975), at excitation by α-particles of the mixture of medium or high pressure (pump power $W \sim 10^{-7}$–10^{-5} W/cm^3) there are no transitions from the M^+N ion levels, which corresponds to the states of atomic ions $M^+(^2P_{3/2})$ (Millet *et al.*, 1981; Khasenov, 2005, 2006). With powerful pumping of an Ar–Xe mixture by the electron beam ($W \sim 1$ MW/cm^3) (Laigle & Collier, 1983) except for the line 329 nm, lines at 345 and 349 nm were observed from the level of Ar^+Xe corresponding to $^2P_{3/2}$ state of Ar^+. Apparently, this was due to mixing of the Ar^+Xe levels at a high electron density.

Emission in 491 nm band is shown in the Kr–Xe mixture at a partial pressure of xenon of several hundred Pa (Fig. 4). At excitation by α-particles of polonium-210, the emission maximum in the 491 nm band was achieved at a Kr:Xe ratio of 1:1. At this ratio of components, approximately 11% of the power enclosed in the gas is converted to radiation in the previously mentioned band (Khasenov, 2005).

4. ATOMIC SPECTRA

In helium, bands of the first negative system of nitrogen (391, 427 nm) were observed and were comparable with the intensity of the 3^1D_2–2^1P_1 transition line (667.8 nm), and weaker lines of helium at 501.6 nm (3^1P_1–2^1S_0), 587.5 nm (3^3D–2^3P), 706.5 nm (3^3S_1–2^3P), and 728.1 nm (3^1S_0–2^1P_1) were also observed.

Atomic lines in argon were only represented by the 4*p*–4*s*-transition (2*p*–1*s* in Paschen notation) lines, and the line at 777.4 nm referred to the atomic oxygen (Fig. 5). Line intensities corrected for the installation spectral sensitivity as well as the total intensity of the transitions from each of the 2*p* levels are shown in Table 1. In cases where the individual lines were outside the range of spectral sensitivity of the installation or were not resolved due to their proximity to stronger line, the total intensity of transitions from the level was determined from the measured intensities of the lines from this level, and the level lifetime value and transition probabilities given in (Radtsig & Smirnov, 1986)

$$I = \frac{I_i}{\tau A_i},$$

https://doi.org/10.1017/S0263034616000616 Published online by Cambridge University Press

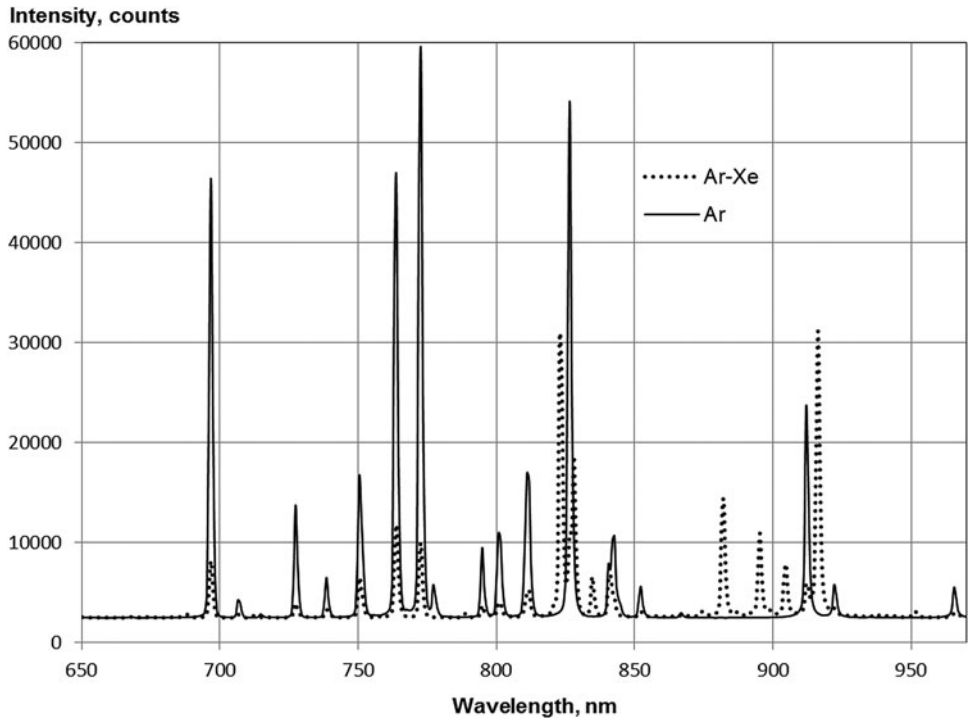

Fig. 5. Spectra of Ar(66.6 kPa) and Ar(65.3 kPa)–Xe(0.67) in the range of 650–975 nm. BK-7 glass lens.

where I_i is the line intensity, A_i is the probability of optical transition, and τ is the level lifetime.

The spectrum of neon emission was dominated by lines from the 3*p*–3*s* transitions of atomic neon (2*p*–1*s* in the Paschen notation, see Table 1) in the near-infrared area of the 3*d*–3*p* transition lines. The atomic oxygen lines at 777.4 and 844.6 nm and a weaker line at 644.5 nm apparently refer to the $5s[3/2]_2$–$3p[3/2]_2$ neon transition were observed. These experiments observed 27 of 30 spectral lines, which are from the 3*p*–3*s* neon atom transitions. The 747.2–868.2 nm regions contain 17 lines due to the 3*d*–3*p* neon transitions, and the total intensity of these lines is 10% of the intensity of the 3*p*–3*s* transitions.

The krypton emission spectrum is dominated by lines of the 5*p*–5*s* transitions of krypton atoms (Fig. 6, Table 2), and there are also very weak lines from the 6*p*–5*s* and the

Table 1. *The intensity lines of the* 2p–1s *transitions of argon (79.6 kPa) and neon (80 kPa) excited by argon ions (relative units, corrected for the spectral sensitivity of the installation)*

Gas	Parameter	$2p_1$	$2p_2$	$2p_3$	$2p_4$	$2p_5$	$2p_6$	$2p_7$	$2p_8$	$2p_9$	$2p_{10}$
Ar	λ	750.4	696.5	706.7	794.8		763.5	772.4	842.5	811.5	912.3
	I	68	218	8	44		266	≈8	75	60	236
	λ		727.3	738.4	852.1		922.4	866.8	801.5		965.8
	I		58	19	26		42	4.5	≈35		63
	λ		772.4	840.8			800.6	810.4			
	I		≈360	33			≈60	45			
	λ		826.5								
	I		437								
	Total	68	1077	60	70	0	373	≈57	115	60	310
Ne	λ	585.1	659.9	607.4	667.8	626.6	614.3	638.3	650.7	640.2	703.2
	I	438	349	161	383	341	385	482	288	411	2556
	λ	540.1	616.4		609.6	671.7	692.9	653.3	633.4		724.5
	I	6	203		268	311	303	180	156		1005
	λ		588.2		594.5	597.6	630.5	621.7	717.4		743.9
	I		143		116	166	61	94	24		274
	λ		603.0								808.2
	I		82								9
	Total	444	777	163	767	830	749	780	468	411	3884

https://doi.org/10.1017/S0263034616000616 Published online by Cambridge University Press

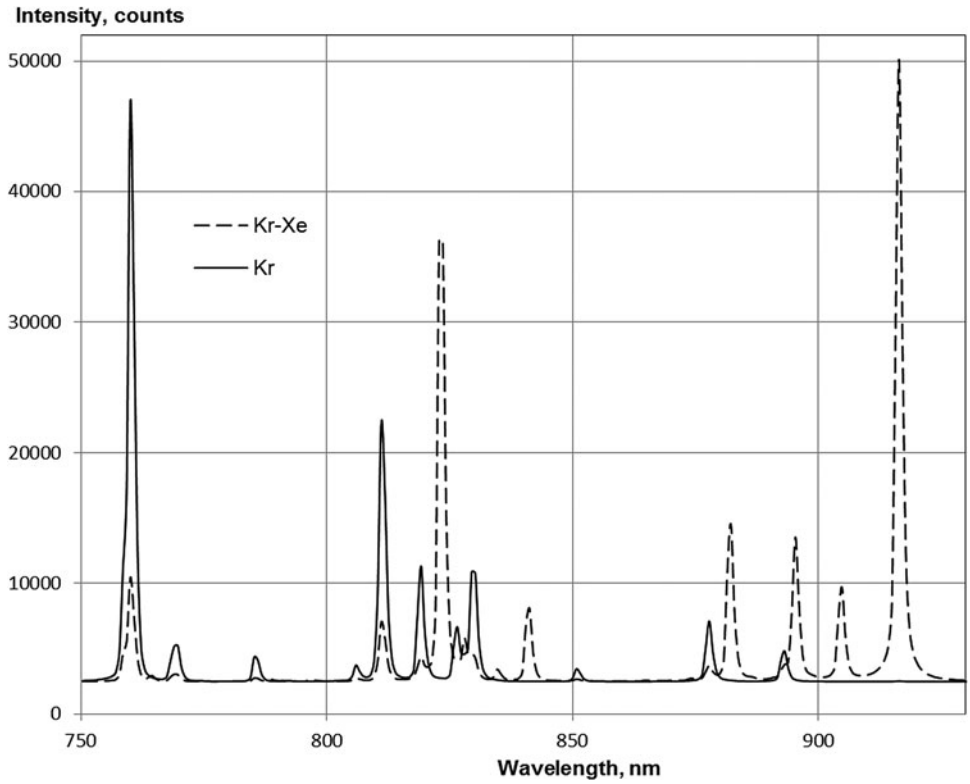

Fig. 6. Spectra of Kr(53.3 kPa) and Kr(52.6 kPa)–Xe(0.67 kPa) in the range of 750–930 nm. Integration time of spectrometer: 1*s*.

Table 2. *The intensity lines of the 2*p*–1*s *transitions of krypton (80.6 kPa), xenon (30.7 kPa), and the lines of xenon in the Kr(52.6 kPa)–Xe(0.67 kPa) and Ar(65.3 kPa)–Xe(0.67 kPa) mixtures excited by argon ions (corrected relative units)*

Gas	Parameter	$2p_1$	$2p_2$	$2p_3$	$2p_4$	$2p_5$	$2p_6$	$2p_7$	$2p_8$	$2p_9$	$2p_{10}$
Kr	λ	768.5	826.3	785.5	806.0		760.2	769.5	877.7	811.3	892.9
	I	10	76	27	19		595	37	110	334	59
	λ		587.1	557.0	850.9		819.0	829.8			
	I		4	4	21		153	155			
	Total	10	80	49[a]	40	~0[b]	648	192	167[c]	334	88
Xe	λ	788.7	764.2	834.7		828.0	823.1	916.3	881.9	904.5	IR
	I	4	9	41		2130	343	226	931	130	
	λ		826.7	473.4			895.2	840.9			
	I		8	1			130	15			
	Total	4	20	42	0	2130	473	241	931	350	
Xe in Kr–Xe	λ		764.2	834.7		828.0	823.1	916.3	881.9	904.5	IR
	I		4	10		37	408	905	193	119	
	λ						895.2	840.9			
	I						170	66			
	Total	0	~8	11	0	37	578	971	193	321	
Xe in Ar–Xe	λ			834.7		828.0	823.1	916.3	881.9	904.5	IR
	I			27		106	168	272	103	51	
	λ						895.2	840.9			
	I						74	29			
	Total	0	0	29	0	106	242	301	103	137	

[a]The 828.1 nm line was not resolved due to the proximity of a strong line at 829.8 nm.
[b]The 758.7 nm line was not resolved due to the proximity of a strong line at 760.2 nm.
[c]The 810.4 nm line was not resolved due to the proximity of a strong line at 811.3 nm.
IR – transitions from the $2p_{10}$ lie outside the spectral sensitivity.

https://doi.org/10.1017/S0263034616000616 Published online by Cambridge University Press

Table 3. *Emission intensity distribution (in percentage) on the* 2p *levels of Xe in the xenon (30.7 kPa), Kr(52.6 kPa)–Xe(0.67 kPa), Ar(65.3 kPa)–Xe(0.67 kPa) mixtures, and* 2p *levels of Kr in the krypton(80.6 kPa) and Ar(59.3 kPa)–Kr(0.67 kPa) mixture*

Gas (mix)	$2p_1$	$2p_2$	$2p_3$	$2p_4$	$2p_5$	$2p_6$	$2p_7$	$2p_8$	$2p_9$	$2p_{10}$
Xe	0.1	0.5	1.0	0	50.8	11.2	5.8	22.2	8.4	IR
Xe in Kr–Xe	0	0.4	0.5	0	1.7	27.4	45.8	9.1	15.1	IR
Xe in Ar–Xe	0	0	3.1	0	11.6	26.4	32.8	11.2	14.9	IR
Kr	0	4.7	2.9	2.4	0	38.7	17.5	9.6	20	4.2
Kr in Ar–Kr	1.4	8.3	3.4	5.7	0	30.0	36.8	12.4	[a]	2.0

[a]The 811.5 nm line was not resolved due to the proximity of an argon line 811.3 nm ($2p_9$–$1s_5$).

6*p*–6*s* transitions of krypton at 427.4 and 432.0 nm, respectively, and the line of krypton's $5d[1/2]_1$–$5p[1/2]_1$ transition (791.3 nm) was also observed.

In the xenon spectrum, in addition to the lines from the 6*p*–6*s* transitions of the xenon atom (see Table 2), there are transitions from the 7*p*, 7*d*, and 5*f* xenon levels demonstrating weak lines with an intensity of one or two relative units. The intensity of the line at 937.5 nm (4*f*–5*d*) was approximately eight relative units, and the total intensity of four lines from the 6*d*–6*p* transitions (890.9, 951.3, 968.5, and 971.8 nm) was 37 units.

A significant difference should be noted between the total intensity of the 2*p*–1*s* transitions for different gases at the same beam power value of the gas:

$$\begin{aligned}&\mathrm{I(Kr,\ 80.6\,kPa):I(Ar,\ 79.6\,kPa):I}\\&\quad\mathrm{(Xe,\ 30,7\,kPa,\ 2}p_{10}\ \mathrm{level\ excluding):I(Ne,\ 80\,kPa)}\\&\quad=1:1.4:2.6:5.7.\end{aligned}$$

The spectra presented in Figures 5 and 6 show the high efficiency of the excitation transfer of argon and krypton to xenon atoms in the Ar–Xe and Kr–Xe mixtures. Nevertheless, the total emission intensity from the 2*p* xenon levels in the Kr–Xe mixture is twofold less than in pure xenon and, for the Ar–Xe mixture, the emission intensity was fourfold less (see Table 2).

5. DICUSSION AND CONCLUSIONS

The results obtained are not sufficient to identify the mechanisms at a level population. It is necessary to further investigate the infrared region of the spectrum and measure the spectral and temporal luminescence characteristics. However, some conclusions can be drawn from these results. The emission intensity distribution at the atomic 2*p* level (see Tables 1–3) is markedly different from the flow of the dissociative recombination of the molecular ions through the levels given in (Ivanov, 1992). To a lesser extent, this applies to neon, and there is a more even distribution of intensity, a higher proportion of transitions from $2p_{10}$ level is explained as a larger share of the recombination flow on this level (22%) and deactivation of the overlying levels by neon. For argon, a noticeable flow portion of the Ar_2^+ dissociative recombination falls on the $2p_9$ level, whereas approximately half of the emission falls on the level $2p_2$. For xenon, the emission partly goes from the level $2p_5$, and this level accounts for only 4% of the Xe_2^+ ion recombination flow. For krypton, 19% of the Kr_2^+ recombination flow falls on the level $2p_2$, and from this level, >5% of photons from the 2*p* levels are emitted. Apparently, the population of the 2*p* levels of the noble gas atoms occurs in the cascade transitions from the *d* levels (Khasenov, 2014; Mel'nikov *et al.*, 2015), and the dissociative recombination of the molecular ions with electrons is not the main process of the 2*p* atomic levels of the noble gas population.

The emission intensity distribution difference in the 2*p* levels for xenon in mixtures with argon and krypton from the distribution in pure xenon may be connected as to the different mechanisms at the population level for pure xenon and its mixtures, and the fact that the rate constant of deactivation of the xenon $2p_5$ level with argon and krypton is 20–30 times greater than the value for atomic xenon (Xu & Setser, 1990).

ACKNOWLEDGMENTS

This work has been supported by the Ministry of Education and Science of the Republic of Kazakhstan (Grant No. 0681/GF4). The author is grateful to staff of the DC-60 accelerator for their assistance in conducting the experiments.

REFERENCES

Abramov, A.A., Gorbunov, V.V., Melnikov, S.P., Mukhamatullin, A.Kh., Pikulev, A.A., Sinitsyn, A.V., Sinyanskii, A.A. & Tsvetkov, V.M. (2006). Luminescence of nuclear-induced rare-gas plasmas in near infrared spectral range. *Proc. SPIE* **6263**, 279–296.

Bennett, W.R. (1962). Optical spectra excited in high pressure noble gases by alpha impact. *Ann. Phys*. **18**, 367–420.

Boichenko, A.M., Tarasenko, V.F., Fomin, E.A. & Yakovlenko, S.I. (1993). Broadband emission continua in rare gases and in mixtures of rare gases with halides. *Quantum Electron*. **23**, 3–25.

Boichenko, A. M., Tarasenko, V. F. & Yakovlenko, S. I. (1999). The nature of third continua in rare gases. *Laser Phys*. **9**, 1004–1020.

Boody, F.P. & Prelas, M.A. (1993). Absolutely calibrated spectra of nuclear-driven rare gases, 400–950 nm. *Proc. Specialist Conf. "The Physics of Nuclear-Excited Plasma and the*

https://doi.org/10.1017/S0263034616000616 Published online by Cambridge University Press

problems of Nuclear-Excited Lasers", Vol. 2, pp. 149–155. Obninsk, Russia.

De Young, R.J. & Weaver, W.R. (1980). Spectra from nuclear-excited plasmas. *J. Opt. Soc. Am*. **70**, 500–506.

Friedl, W. (1959). Krypton-Xenon Banden. *Z. Naturforsch*. **14A**, 848–848a.

Gikal, B., Dmitriev, S., Apel, P., Bogomolov, S., Borisov, O., Buzmakov, V., Gulbekyan, G., Ivanenko, I., Ivanov, O., Itkis, M., Kazarinov, N., Kalagin, I., Kolesov, I., Papash, A., Paschenko, S., Tikhomirov, A. & Khabarov, M. (2008). DC-60 heavy ion cyclotron complex: The first beams and project parameters. *Phys. Part. Nucl. Lett*. **5**, 642–644.

Gorbunov, V.V., Grigor'ev, V.D., Dovbysh, L.E., Mel'nikov, S.P., Sinitsyn, A.V., Sinjanskii, A.A. & Tsvetkov, V.M. (2004). The luminescence spectra in the 350–875 nm range of the dense gas excited by uranium fission fragments. *Proc. RFNC-VNIIEF*, Issue 6, pp. 148–173 (in Russian).

Griegel, T., Drotleff, H.W., Hammer, J.W. & Petkau, K. (1990). The third continuum of the rare gases emitted by heavy ion beam induced plasmas. *J. Chem. Phys*. **93**, 4581–4588.

Ivanov, V.A. (1992). Dissociative recombination of molecular ions in noble-gas plasmas. *Sov. Phys. – Usp*. **35**, 17–36.

Khasenov, M.U. (2005). Emission of ionic molecules $(KrXe)^+$ at excitation by a hard ionizer. *J. Appl. Spectrosc*. **72**, 316–320.

Khasenov, M.U. (2006). Emission of the heteronuclear ionic molecules $(ArXe)^+$ at excitation by a hard ionizer. *Proc. SPIE* **6263**, 141–148.

Khasenov, M.U. (2014). Mechanisms of population of the levels in gas lasers pumped by ionizing radiation. *Laser Part. Beams* **32**, 501–508.

Kugler, E. (1964). Über die Lumineszenze der Edelgasgemische Ar/Xe, Kr/Xe, Ar/Kr und der Gemische Xe/N_2 und Kr/N_2 bei Angerung mit schnellen Elektronen. *Ann. Phys., Leipzig* **14**, 137–146.

Laigle, C. & Collier, F. (1983). Kinetic study of $(ArXe)^+$ heteronuclear ion in electron beam excited Ar–Xe mixture. *J. Phys. Ser. B* **16**, 687–697.

McCusker, M. (1984). The rare gas excimers. In *Excimer Lasers*. 2nd edn. (Rhodes, C.K., Ed.), pp. 47–86. Berlin: Springer-Verlag.

Mel'nikov, S.P., Sizov, A.N., Sinyanskii, A.A. & Miley, G.H. (2015). *Lasers with Nuclear Pumping*. Heidelberg: Springer.

Millet, P., Barrie, A.M., Birot, A., Brunet, H., Dijols, H., Galy, G. & Salamero, J. (1981). Kinetic study of $(ArKr)^+$ and $(ArXe)^+$ heteronuclear ion emissions. *J. Phys., Ser. B* **14**, 459–472.

Mis'kevich, A.I. (1991). Visible and near-infrared direct nuclear pumped lasers. *Laser Phys*. **1**, 445–481.

Prelas, M.A., Boody, F. P., Miley, G.H. & Kunze, J. F. (1988). Nuclear driven flashlamps. *Laser Part. Beams* **6**, 25–62.

Radtsig, A.A. & Smirnov, B.M. (1986). *Parameters of Atoms and Atomic Ions*. Moscow: Energoatomizdat (in Russian).

Sakasai, K., Kakuta, T., Yamagishi, H., Nakazawa, M., Yamanaka, N. & Iguchi, T. (1996). Experiments for optical neutron detection using nuclear pumped laser. *IEEE Trans. Nucl. Sci*. **43**, 1549–1553.

Tanaka, Y., Yoshino, K. & Freeman, D.E. (1975). Emission spectra of heteronuclear diatomic rare gas positive ions. *J. Chem. Phys*. **62**, 4484–4496.

Ulrich, A. (2012). Light emission from the particle beam induced plasma: An overview. *Laser Part. Beams* **30**, 199–205.

Ulrich, A., Adonin, A., Jacoby, J., Turtikov, V., Fernengel, D., Fertman, A., Golubev, A., Hoffmann, D.H.H., Hug, A., Krucken, R., Kulish, M., Menzel, J., Morozov, A., Ni, P., Nikolaev, D.N., Shilkin, N.S., Ternovoi, V.Ya., Udrea, S., Varentsov, D. & Wieser, J. (2006). Excimer laser pumped by an intense, high-energy heavy-ion beam. *Phys. Rev. Lett*. **97**, 153901.

Wieser, J., Ulrich, A., Fedenev, A. & Salvermoser, M. (2000). New interpretation of the third rare gas excimer continua. *Proc. SPIE* **4071**, 248–254.

Xu, J. & Setser, D.W. (1990). Deactivation rate constants and product branching in collisions of the Xe(6p) states with Kr and Ar. *J. Chem. Phys*. **92**, 4191–4202.

Zdorovets, M., Ivanov, I., Koloberdin, M., Kozin, S., Alexandrenko, V., Sambaev, E., Kurakhmedov, A. & Ryskulov, A. (2014). Accelerator complex based on DC-60 cyclotron. *Proc. 24th Russian Particle Accelerator Conf*., pp. 287–289. Obninsk: FEI.